

## Wavelength-Modulation Spectra of Some Semiconductors

RICARDO R. L. ZUCCA\* AND Y. R. SHEN

*Department of Physics, University of California and Inorganic Materials Research Division,  
Lawrence Radiation Laboratory, Berkeley, California 94720*

(Received 20 October 1969)

Wavelength-modulation spectra of GaAs, GaSb, InAs, InSb, Ge, and Si at 5, 80, and 300°K are presented. The spectral range extends from 1.75 to 6.0 eV. The results are compared with electroreflectance and thermorefectance data. New structures are found in the spectra of all crystals. With the help of existing band structures of these crystals, all the reflectivity peaks can be consistently assigned to proper critical transitions between the valence and the conduction bands. Values of spin-orbit splittings at several symmetry points can be calculated. Temperature effects on the band spectra are discussed.

### I. INTRODUCTION

IN recent years, the subject of band structures of semiconductors has attracted much attention. Theoretically, the introduction of the empirical pseudopotential method<sup>1</sup> has led to a much better understanding of the band structures. Further progress requires improvement on the resolution of empirical spectra. Experimentally, the application of optical derivative spectroscopy to solids has greatly improved the resolution of optical spectra. The results have had strong impact on the recent advance in band-structure calculations.

Many different modulation schemes have been invented for derivative spectroscopy. For measurements of reflectivity spectra of solids, electroreflectance,<sup>2</sup> piezorefectance,<sup>3-5</sup> thermorefectance,<sup>6,7</sup> and wavelength-modulation<sup>8</sup> methods have been most successful. In all these schemes except the wavelength-modulation method, modulation of the light beam is obtained through application of a direct ac perturbation on the solid, and, hence, interpretation of the derivative spectrum depends very much on how the solid responds to the perturbation. Thus, in electroreflectance, we must know how the band structure of the solid changes with an applied electric field. In piezorefectance and thermorefectance, we must know the variation of the band structure as a function of pressure and temperature, respectively. Unfortunately, our knowledge on such properties of a solid is generally rather limited. Therefore, the fact that no perturbation on the solid is needed makes the wavelength-modulation method most attractive. Since the wavelength-modulation spectrum is

simply the derivative of the normal spectrum, there is no ambiguity in the interpretation.

However, unlike the other modulation schemes, the wavelength-modulation method requires careful construction of the experimental system in order to eliminate the huge background in the derivative spectrum. This background appears as a result of wavelength modulation on the spectra of various optical components in the system. In particular, because of the many narrow spectral lines in the arc source, it is difficult to apply the scheme to the uv region. For this reason, the wavelength-modulation method has not been as popular as the other modulation schemes. Work done with wavelength modulation has usually been limited to a narrow region in the visible or near infrared.<sup>9-11</sup>

Recently, we have succeeded in constructing a wavelength-modulation spectrometer which practically eliminates all the background. On the other hand, the sensitivity of the spectrometer is still as high as  $\Delta R/R \cong 10^{-4}$ . We have used this spectrometer to obtain derivative spectra of Si, Ge, GaAs, GaSb, InAs, and InSb from 1.75 to 6 eV. In order to resolve fine structures in the spectra, we have made measurements at liquid-nitrogen and liquid-helium temperatures. In this paper, we would like to present the results of our investigation. While the gross features of our spectra agree with the results of others,<sup>3,7</sup> new structures and more fine details appear in our spectra, particularly in the uv region.

In the following section, a brief description of the experimental arrangement is first given. Then, in Sec. III, the wavelength-modulation spectra of the six semiconductors at 5, 80, and 300°K are presented. In Sec. IV, the derivative spectra are analyzed with the help of the existing band structures of semiconductors, various reflectivity peaks are assigned to proper critical transitions between bands. Emphasis is on the new structures we have observed. Variation of the derivative spectra with temperature is discussed qualitatively.

\* Fellow, Consejo Nacional de Investigaciones Cientificas y Tecnicas, Argentina.

<sup>1</sup> M. L. Cohen and V. Heine, in *Solid State Physics*, edited by F. Seitz, D. Turnbull, and H. Ehrenreich (Academic Press Inc., New York, to be published), and references therein.

<sup>2</sup> B. O. Seraphin and N. Bottka, *Phys. Rev.* **145**, 628 (1966).

<sup>3</sup> M. Cardona, K. Shaklee, and F. H. Pollak, *Phys. Rev.* **154**, 696 (1967).

<sup>4</sup> W. E. Engeler, H. Fritzsche, M. Garfinkel, and J. J. Tiemann, *Phys. Rev. Letters* **14**, 1069 (1965); M. Garfinkel, J. J. Tiemann, and W. E. Engeler, *Phys. Rev.* **148**, 695 (1966).

<sup>5</sup> G. W. Gobeli and E. O. Kane, *Phys. Rev. Letters* **15**, 142 (1965).

<sup>6</sup> B. Batz, *Solid State Commun.* **4**, 241 (1966).

<sup>7</sup> M. Matatagui, A. G. Thompson, and M. Cardona, *Phys. Rev.* **176**, 950 (1968).

<sup>8</sup> See, for example, I. Balslev, *Phys. Rev.* **143**, 636 (1966).

<sup>9</sup> K. L. Shaklee, J. E. Rowe, and M. Cardona, *Phys. Rev.* **174**, 828 (1968).

<sup>10</sup> J. E. Rowe, M. Cardona, and K. L. Shaklee, *Solid State Commun.* **7**, 441 (1969).

<sup>11</sup> J. E. Rowe, F. H. Pollak, and M. Cardona, *Phys. Rev. Letters* **22**, 933 (1969).

## II. EXPERIMENTAL ARRANGEMENT

### A. Spectrometer

The construction of our wavelength-modulation spectrometer follows mainly the design of French *et al.*<sup>12</sup> with only slight modifications. Here, we shall give only a brief account of it. Wavelength modulation was achieved through vibration of a mirror in the optical path inside the spectrometer. A double-beam method was used to eliminate the background in the derivative spectrum. One beam had its dc and ac outputs proportional to  $I_0$  and  $\Delta I_0/\Delta\lambda$ , respectively, and the other had outputs proportional to  $I_0R$  and  $\Delta(I_0R)/\Delta\lambda$ , respectively, where  $I_0$  is the beam intensity in the absence of the sample and  $R$  is the reflectivity of the sample. Two of the outputs were used to control two feedback loops, making  $\Delta I_0/\Delta\lambda=0$  and  $I_0=\text{constant}$  (or  $I_0R=\text{const}$ ). The other two outputs then gave the signals  $\Delta R/\Delta\lambda$  and  $R$  (or  $\Delta R/R\Delta\lambda$  and  $1/R$ ).

Maximum slit width and modulation amplitude were chosen with precaution such that line shapes of the fine structures in the derivative spectrum were not distorted. The sharpest structure in our spectra had a width larger than 60 Å. The derivative spectrum  $\Delta R(\lambda)/R\Delta\lambda$  versus  $\lambda$  was recorded by a chart recorder. A simple computer program was then used to convert the spectrum to  $\Delta R(E)/R\Delta E$  versus the energy  $\Gamma$  in eV. The conversion makes the structures at higher frequencies less pronounced, but the corresponding noise amplitude also decreases proportionally. Therefore, small wiggles in the uv region of our spectra  $\Delta R/R\Delta E$  versus  $E$  deserve full attention as true structure.

In order to make sure that the observed structure of the spectrum were characteristics of the sample rather than other spurious effects, we used the spectrum of aluminum as a reference. Aluminum was chosen because its spectrum shows little structure in the region in which we were interested.

### B. Dewar

The optical Dewar was manufactured by Janis Research Company. Temperature of the sample can be varied continuously from the liquid-helium temperature to the room temperature. The temperature control has a long-term stability of better than 1°K/h. A copper-constantan thermocouple was used to measure the temperature over the whole range of interest with an accuracy of  $\pm 1^\circ\text{K}$ . This was sufficient for our purpose since the spectrum changes gradually with temperature. Most of our spectra were taken at 5, 80, and 300°K.

### C. Samples

All the samples we measured were wafers of single crystals with (1,1,1) orientation. The samples were

polished and etched following the standard procedure.<sup>13</sup> For good reproducibility, a crystal surface free of mechanical distortion and chemical contamination was essential.<sup>3</sup> Surface contamination often produced more distortion of the spectrum in the uv than in the visible. All our measurements were made on freshly prepared samples.

The samples were of either *n*- or *p*-type, doped with a carrier concentration in the range between  $10^{13}$  and  $10^{17}$  cm<sup>-3</sup>. We would expect that the wavelength-modulation spectrum is independent of the carrier concentration. This was confirmed by measurements on two samples of Si with carrier concentrations of  $10^{13}$  and  $10^{17}$  cm<sup>-3</sup>, respectively.

## III. EXPERIMENTAL RESULTS

In Fig. 1, we show a derivative spectrum  $\Delta R(E)/R\Delta E$  of InSb at 5°K, together with the normal reflectivity spectrum  $R(E)$ . That the derivative spectrum has a better resolution is clearly shown. Differentiation of  $R(E)$  on a computer yields the same derivative spectrum, but with a much smaller signal-to-noise ratio.

In Figs. 2–7, we present the derivative spectra,  $\Delta R(E)/R\Delta E$  of GaAs, GaSb, InAs, InSb, Ge, and Si, respectively, at three different temperatures, 5, 80, and 300°K. Compared with the derivative spectra obtained from electroreflectance<sup>3</sup> and thermorelectance<sup>7</sup> measurements, our spectra give the same gross feature, but show definite improvement with more fine structures, especially at low temperatures. As an example, we reproduce in Figs. 4(b) and 4(c), respectively, the electroreflectance and the thermorelectance spectra of InAs obtained by Cardona *et al.*<sup>3,7</sup> The temperature variation of the wavelength-modulation spectra is fairly striking, although the change is rather gradual. All the main structures shifted to higher energies when the tempera-

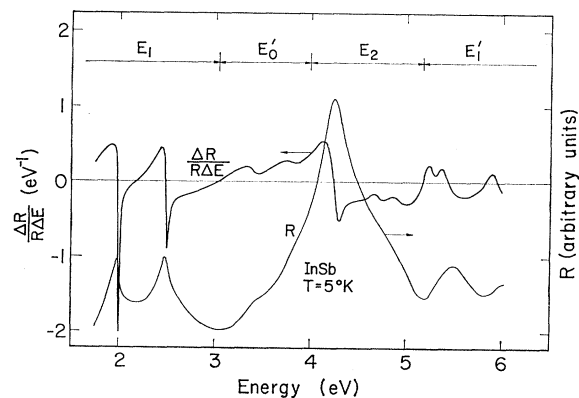


FIG. 1. Reflectivity spectrum and logarithmic derivative reflectivity spectrum of InSb at 5°K in the range between 1.75 and 6 eV.

<sup>12</sup> C. S. French and A. B. Church, *Carnegie Institution of Washington Yearbook* **54**, 162 (1954); **56**, 281 (1956); Ricardo R. L. Zucca and Y. R. Shen (unpublished).

<sup>13</sup> H. C. Gatos and M. C. Levine, in *Progress in Semiconductors*, edited by A. F. Gibson and R. E. Burgess (Temple Press, London, 1965), Vol. 9, p. 1.

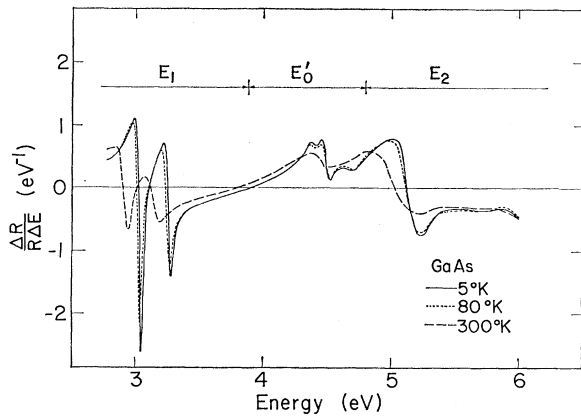


FIG. 2. Logarithmic derivative of the reflectivity spectrum of GaAs at 5, 80, and 300°K.

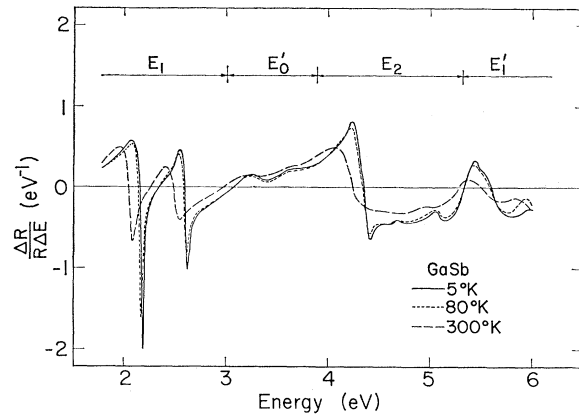
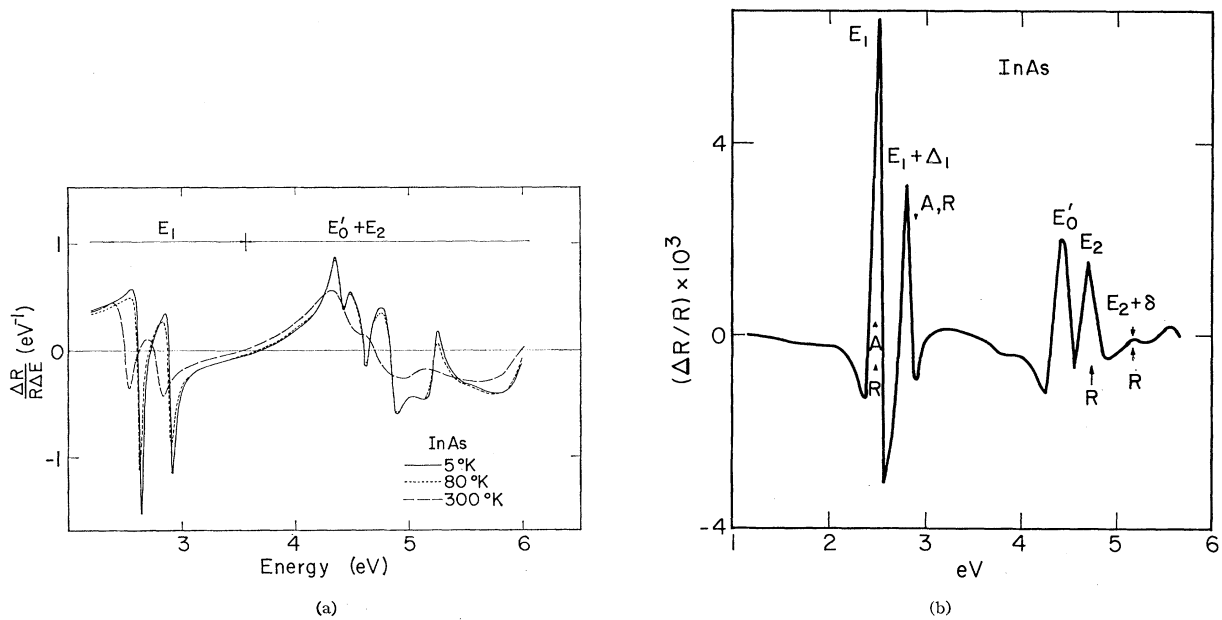
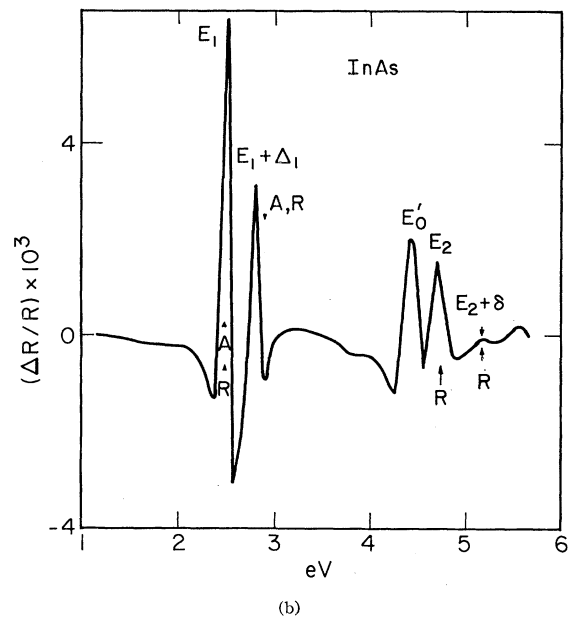


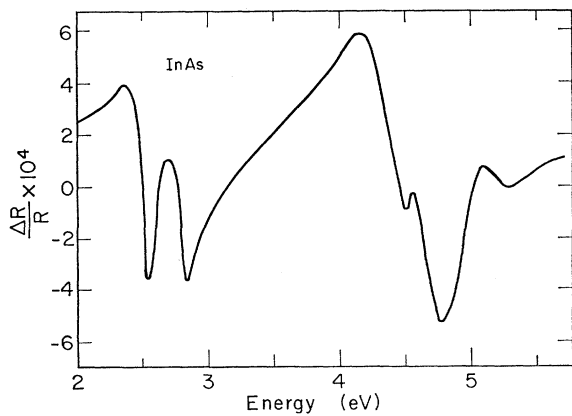
FIG. 3. Logarithmic derivative of the reflectivity spectrum of GaSb at 5, 80, and 300°K.



(a)



(b)



(c)

FIG. 4. (a) Logarithmic derivative of the reflectivity spectrum of InAs at 5, 80, and 300°K. (b) Electroreflectance spectrum of InAs at room temperature (reproduced from Ref. 3). (c) Thermoreflectance spectrum of InAs at 77°K (reproduced from Ref. 7).

ture is lowered. The structures generally become sharper at lower temperatures.

The spectra of the six crystals are very much alike, reflecting the similarity of their band structures. Following partially the notations of Cardona *et al.*,<sup>3</sup> we divide the structures in each spectrum into groups, labelled by  $E_0$ ,  $E_1$ ,  $E_0'$ ,  $E_1'$ , etc., as shown in the figures. Similar groups (having the same label) in different semiconductors are believed to come from transitions in the similar general areas of the band structures. The group  $E_0$ , corresponding to transitions near the direct fundamental-energy gap, has not been covered by our experiments.

As shown in Figs. 2-7, each group may contain many structures. These structures presumably come from several reflectivity peaks superimposed on top of one another. Decomposition of a composite line into individual peaks is always somewhat arbitrary. In our case, the decomposition was made with the following general rules: (1) The low-temperature spectrum of a composite line should be decomposed into a minimum number of individual lines with simple line shapes. (2) Recomposition of these individual lines with broadened linewidths should yield the high-temperature spectrum of the composite line. (3) Similarity in the spectra of different semiconductors should be used as a guide line in the decomposition.

With these rules, we found little ambiguity in decomposing our spectra although the positions of the components may not be very accurate and their shapes somewhat arbitrary. An example of the decomposition is shown in Fig. 8. In Table I, we list the positions of all the reflectivity peaks obtained from decomposition of our spectra at 5°K for the six semiconductors. The accuracy of the most uncertain values in the table is estimated to be better than  $\pm 0.03$  eV.

We now proceed to comment briefly on the low-temperature spectrum of each semiconductor separately.

*GaAs* (Fig. 2). Although the spectrum below 2.7 eV

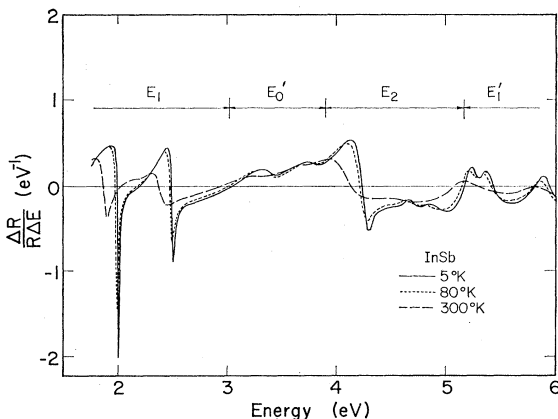


FIG. 5. Logarithmic derivative of the reflectivity spectrum of InSb at 5, 80, and 300°K.

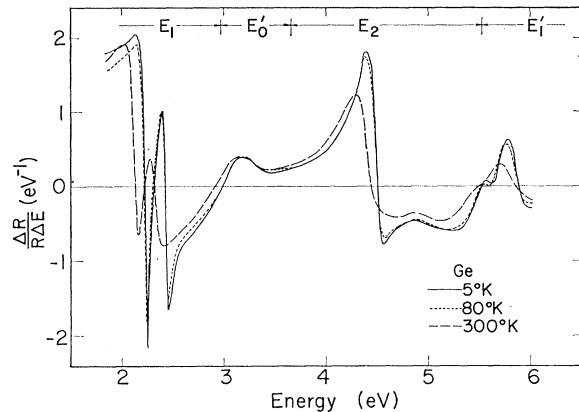


FIG. 6. Logarithmic derivative of the reflectivity spectrum of Ge at 5, 80, and 300°K.

is not shown in Fig. 2, we have explored this region carefully. We have not been able to find the small structures at 2.3 and 2.6 eV observed by Greenaway.<sup>14</sup> In the  $E_1$  region, our spectrum confirms the absence of the small structures suggested by Lukes *et al.*<sup>15</sup> Decomposition of the spectrum in the  $E_0'$  region yields two reflectivity peaks. Decomposition in the  $E_2$  region is somewhat arbitrary. To be consistent with the spectra of other III-V compounds, we should decompose the  $E_2$  group into a strong broad peak with three small peaks at higher energies. Part of the  $E_2$  spectrum above 6 eV was cut off by our spectrometer.

*GaSb* (Fig. 3). The structure at 1.9 eV observed by Greenaway<sup>14</sup> is absent in our spectrum. Decomposition of the spectrum gives unambiguously two peaks in the  $E_0'$  region, one strong and three weak in the  $E_2$  region,

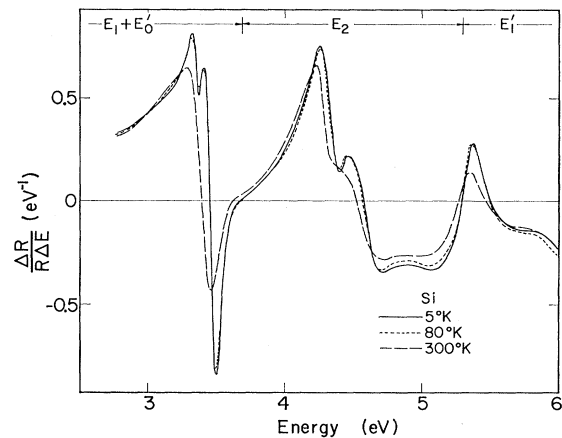


FIG. 7. Logarithmic derivative of the reflectivity spectrum of Si at 5, 80, and 300°K.

<sup>14</sup> D. L. Greenaway, Phys. Rev. Letters 9, 97 (1962); D. L. Greenaway and M. Cardona, in *Proceedings of the International Conference on the Physics of Semiconductors, Exeter* (The Institute of Physics and the Physical Society, London, 1962), p. 666.

<sup>15</sup> F. Lukes and E. Schmidt, in *Proceedings of the International Conference on the Physics of Semiconductors, Exeter* (The Institute of Physics and the Physical Society, London, 1962), p. 389.

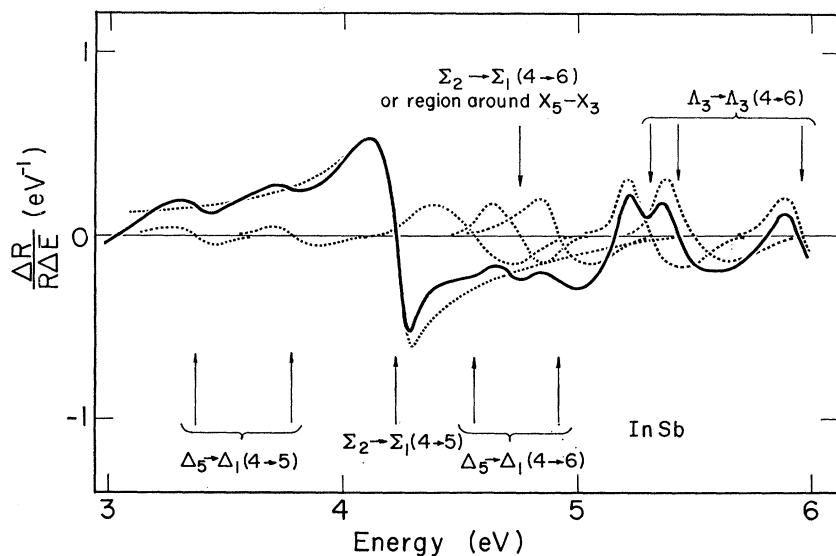


FIG. 8. Decomposition of the derivative reflectivity spectrum of InSb at 5°K into many components according to the general rules stated in the text.

and two in the  $E_1'$  region. The shape of the spectrum near 6 eV indicates the presence of additional structures just above 6 eV belonging to the  $E_1'$  group.

*InAs* (Fig. 4). We cannot identify in our spectrum the peaks at 2.2 and 2.45 eV suggested by Greenaway.<sup>14</sup> The spectrum of InAs is somewhat different from those of other III-V compounds in the sense that the  $E_0'$  and the  $E_2$  regions overlap. We can unambiguously decompose the structures in this  $E_0'+E_2$  region into six reflectivity peaks. We assign the two weak ones at lower frequencies to the  $E_0'$  group and the rest to the  $E_2$  group. Note that the spectrum of InAs appears to have a very strong temperature dependence.

*InSb* (Fig. 5). The spectrum of InSb looks very much similar to that of GaSb. Decomposition of the spectrum gives two peaks in the  $E_0'$  region, four in the  $E_2$  region, and three in the  $E_1'$  region.

*Ge* (Fig. 6). The spectrum of Ge is still quite similar to those of III-V compounds, but with less structure. Decomposition of the spectrum yields one peak in the  $E_0'$  region, one strong and one weak in the  $E_2$  region, and two in the  $E_1'$  region.

*Si* (Fig. 7). Because of the difference in the band structures near the direct gap, the spectrum of Si is somewhat different from those of others in the  $E_1$  and  $E_0'$  regions. Here, the  $E_1$  peak appears at higher energy and overlaps with the  $E_0'$  peak. We assign the peak at 3.4 eV to  $E_0'$ , and the one at 3.45 eV to  $E_1$ . The spectrum in the  $E_2$  and  $E_1'$  regions are similar to those of others. We can decompose the spectrum into one strong and one weak peak in the  $E_2$  region, and one in the  $E_1'$  region.

#### IV. DISCUSSION

A qualitative comparison between our spectra and the spectra obtained from electroreflectance<sup>2,3</sup> and thermoreflectance<sup>6,7</sup> measurements should be made. At room temperature, our spectra compare well with thermoreflectance spectra. The electroreflectance spectra generally show more structures, but the assignment of electroreflectivity peaks is somewhat arbitrary. Our low-temperature spectra appear better resolved than either thermoreflectance or electroreflectance spectra. While we recognize no new structure in the  $E_1$  region,

TABLE I. Energies (eV) of observed reflectivity peaks in the six crystals. Assignment of various peaks to particular interband transitions is also given.

	$E_1$		$E_0'$		$E_2$			$E_1'$			
	$\Lambda_3 \rightarrow \Lambda_1$		$\Delta_5 \rightarrow \Delta_1$ (4→5)		$\Sigma_2 \rightarrow \Sigma_1$ (4→5)	$\Sigma_2 \rightarrow \Sigma_1$ (4→6) or around $X_5 \rightarrow X_3$	$\Delta_5 \rightarrow \Delta_1$ (4→6)		$\Lambda_3 \rightarrow \Lambda_3$		
GaAs	3.017	3.245	4.44	4.60	5.11	5.64(?)	5.91	6.07(?)			
GaSb	2.154	2.596	3.35	3.69	4.35	4.55	4.75	5.07	5.51	5.65	
InAs	2.612	2.879	4.39	4.58	4.74	4.85	5.31	5.50			
InSb	1.983	2.478	3.39	3.78	4.23	4.75	4.56	4.92	5.33	5.50	5.96
Ge		2.222		3.20		4.49		5.01		5.65	5.88
Si		3.45		3.40		4.44		4.60		5.50	
Estimated uncertainty	±0.004		±0.008		±0.01	±0.03	±0.03		±0.03		

TABLE II. Spin-orbit splittings (in eV) at various points in the band structures of the six crystals, obtained from analysis of our reflectivity spectra. The values of spin-orbit splittings at  $\Gamma_{15}$  are obtained from the reference M. Cardona, K. L. Shaklee, and F. H. Pollak, Phys. Rev. **154**, 696 (1967).

Material \ S-o splitting at	$\Gamma_{15}$	$\Lambda_3(4)$		$\Lambda_3(6)$	$\Delta_5$	
		From $\Lambda_3 \rightarrow \Lambda_1$ transitions	From $\Delta_3 \rightarrow \Delta_3$ transitions		From $\Delta_5 \rightarrow \Delta_1$ ( $4 \rightarrow 5$ ) transitions	From $\Delta_5 \rightarrow \Delta_1$ ( $4 \rightarrow 6$ ) transitions
GaAs	0.34	0.22		0.14	0.16	0.16(estimate)
GaSb	0.80	0.45			0.34	0.32
InAs	0.43	0.27		0.17	0.19	0.19
InSb	0.82	0.50	0.63		0.39	0.36
Ge	0.29	0.20	0.23			
Si	0.04					

there are generally more distinct structures in  $E_0'$ ,  $E_2$ , and  $E_1'$  regions.

We must now identify the various reflectivity peaks in our spectra with particular interband transitions in the crystals. Normally, a reflectivity peak which is originated from an absorption peak comes from interband transitions in the region around a critical point of high symmetry.<sup>16</sup> Here, we shall use this as a general principle in the assignment of reflectivity peaks.

For the purpose of illustration, we reproduce in Fig. 9 the band structure of GaSb.<sup>1,17</sup> The band structures of the other semiconductors, except Si, are qualitatively similar to that of GaSb. For Si, the point  $\Gamma_1(\Gamma_2')$  appears to be higher in energy than  $\Gamma_{15}$ . (We use here the zincblende group notations for Si and Ge.) The band structure of Fig. 9 should be modified accordingly.<sup>18</sup> A direct consequence is that Si has an indirect energy gap along  $\Delta$ . In Fig. 9, we use arrows to indicate critical transitions with large joint densities of states in those general areas of the Brillouin zone. These are the transitions which may give rise to the observed reflectivity peaks. Recent calculations indicate that a reflectivity peak can occasionally come from interband transitions over a region away from any critical point of high symmetry.<sup>1,19</sup> However, reflectivity peaks due to such transitions can only be identified through calculation of optical transitions over the whole Brillouin zone. We must, therefore, regard our assignment here as only preliminary.

Let us now discuss each spectral region separately for the six crystals. Assignment of all the observed reflectivity peaks to the corresponding interband transitions is summarized in Table I. Our assignment is based on the available information about the band structures of these semiconductors.<sup>1,16-24</sup> Unless specified, we shall always refer to the spectra at 5°K.

<sup>16</sup> J. C. Phillips, in *Solid State Physics*, edited by F. Seitz and D. Turnbull (Academic Press Inc., New York, 1966), Vol. 18, p. 55.

<sup>17</sup> R. Cahn and M. L. Cohen, Phys. Rev. (to be published).

<sup>18</sup> M. L. Cohen and T. K. Bergstresser, Phys. Rev. **141**, 789 (1966).

<sup>19</sup> E. O. Kane, Phys. Rev. **146**, 558 (1966).

<sup>20</sup> J. P. Walter and M. L. Cohen, Phys. Rev. **183**, 763 (1969).

<sup>21</sup> H. I. Zhang and J. Callaway, Phys. Rev. **181**, 1163 (1969).

<sup>22</sup> F. H. Pollak, C. W. Higginbotham, and M. Cardona, J. Phys. Soc. Japan Suppl. **21**, 20 (1966).

<sup>23</sup> F. Herman, R. L. Kortum, D. C. Kuglin, J. P. Van Dyke, and

### A. $E_1$ Region

Except for Si, all our spectra show a sharp doublet. It is generally agreed that this doublet corresponds to  $\Lambda_3 \rightarrow \Lambda_1$  transitions with the  $\Lambda_3$  level spin-orbit split.<sup>1,3</sup> A simple analysis<sup>24</sup> shows that the spin-orbit splitting of  $\Lambda_3$  near  $L$  should be around  $\frac{2}{3}$  of the spin-orbit splitting at  $\Gamma_{15}$ . No spin-orbit splitting should exist for the  $\Lambda_1$  level.<sup>25</sup> As shown in Table II, the observed splitting of the doublet confirms the above  $\frac{2}{3}$  rule.

The nonexistence of reflectivity peaks for  $L_3 \rightarrow L_1$  transitions has been a mystery.<sup>1,14</sup> The fact that we have seen no additional structure in the  $E_1$  region indicates that either the  $L_3 \rightarrow L_1$  transitions are too weak or they are hidden in the  $\Lambda_3 \rightarrow \Lambda_1$  structure.

The band structure of Si puts  $\Gamma_1(\Gamma_2')$  above  $\Gamma_{15}$ . This makes the  $\Lambda_3 \rightarrow \Lambda_1$  transitions and the  $\Delta_5 \rightarrow \Delta_1(4-5)$  transitions partially degenerate in energy.<sup>18</sup> As shown in Fig. 7, there are two overlapping reflectivity peaks at 3.40 and 3.45 eV. Assuming that similar transitions in different crystals would yield reflectivity peaks of similar strength, we should assign the 3.45 eV peak to the  $\Lambda_3 \rightarrow \Lambda_1$  transitions, and the 3.40 eV peak to the

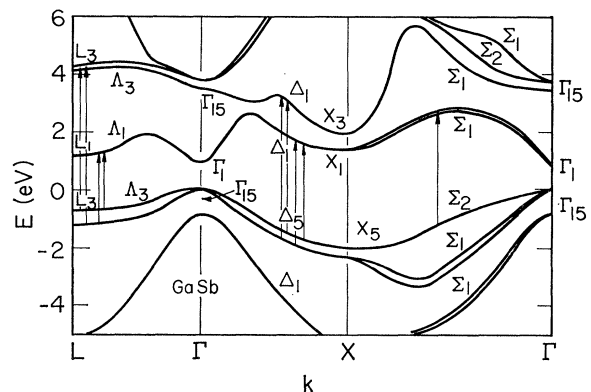


FIG. 9. Band structure of GaSb (reproduced from Ref. 1). Arrows indicate interband transitions which are possibly responsible for the observed reflectivity peaks.

S. Skillman, in *Methods of Computational Physics*, edited by B. Alder, S. Fernbach, and M. Rotenberg (Academic Press Inc., New York, 1968), Vol. 8, 193.

<sup>24</sup> L. R. Savavia and D. Brust, Phys. Rev. **176**, 915 (1968).

<sup>25</sup> R. H. Parmenter, Phys. Rev. **100**, 573 (1955).

$\Delta_5 \rightarrow \Delta_1$  (4-5) transitions. The spin-orbit coupling in Si is small. It gives a splitting of 0.04 eV at  $\Gamma_{15}(\Gamma_{25}')$ ,<sup>3,26</sup> and even smaller splittings along  $\Lambda_3$  and  $\Delta_5$ .<sup>24</sup> The resolution of our Si spectrum is clearly not sufficient to show the spin-orbit splitting of either  $\Lambda_3 \rightarrow \Lambda_1$  or  $\Delta_5 \rightarrow \Delta_1$  (4-5) transitions. We, therefore, rule out the possibility that the two peaks at 3.40 and 3.45 eV could correspond to the spin-orbit doublet of the  $\Lambda_3 \rightarrow \Lambda_1$  transitions.

Figures 2-7 show that all the  $E_1$  peaks appear significantly sharper at lower temperatures. This suggests possible exciton effects associated with the  $\Lambda_3 \rightarrow \Lambda_1$  transitions. Shaklee *et al.*<sup>9</sup> have shown that the existence of hyperbolic excitons at  $\Lambda$  can explain the observed lineshape of the  $E_1$  peaks. Rowe *et al.*<sup>11</sup> have also confirmed the existence of hyperbolic excitons from the pressure dependence of the  $E_1$  peaks. Our spectra suggest that this exciton effect is present in all III-V and group-IV semiconductors.

### B. $E_0'$ Region

We can identify a doublet in the  $E_0'$  group for the four III-V compounds and a single peak for the two group-IV elements. These  $E_0'$  peaks were originally assigned to 4-5 transitions at or near  $\Gamma$ ,<sup>3,14</sup> but the low joint density of states near  $\Gamma$  rules out such an assignment.<sup>17,20</sup> The peaks are more likely due to  $\Delta_5 \rightarrow \Delta_1$  (4-5) transitions away from  $\Gamma$ .<sup>17,20</sup> Only the  $\Delta_5$  level is spin-orbit split. Pseudopotential<sup>17,26</sup> and  $\mathbf{k} \cdot \mathbf{p}$  calculations<sup>22</sup> indicate that the spin-orbit splitting along  $\Delta_5$  should be even smaller than the splitting at  $L_3$  (band 4) (which is  $\frac{2}{3}$  of the splitting at  $\Gamma_{15}$ ). Our results agree well with this assertion. The observed  $E_0'$  doublet for III-V compound has indeed a splitting smaller than that of the  $E_1$  doublet (see Table II). In Ge, the symmetry points at  $X_5$  become degenerate, and calculation shows that the spin-orbit splitting along  $\Delta_5(4)$  should be small.<sup>24</sup> We would not expect to resolve the spin-orbit doublet in the Ge spectrum. We should, therefore, assign the single  $E_0'$  peak of Ge to  $\Delta_5 \rightarrow \Delta_1$  (4-5) transitions. The same is true for Si, which has even smaller spin-orbit coupling.

### C. $E_2$ Region

Our spectra for all the six crystals seem rather complicated in this region. They generally show more structure than either electroreflectance or thermoreflectance spectra. However, we can always decompose the  $E_2$  group quite unambiguously into a broad strong reflectivity peak and several small peaks at higher energies. Pseudopotential calculation<sup>1,17,19</sup> indicates that this broad peak should be due to  $\Sigma_2 \rightarrow \Sigma_1$  (4  $\rightarrow$  5) transitions over a large region in the Brillouin zone. The spin-orbit splitting along  $\Sigma_1$  is small<sup>17,23</sup> and would be difficult to resolve. From the band structure of Fig. 10, one might expect to observe a reflectivity peak corresponding to

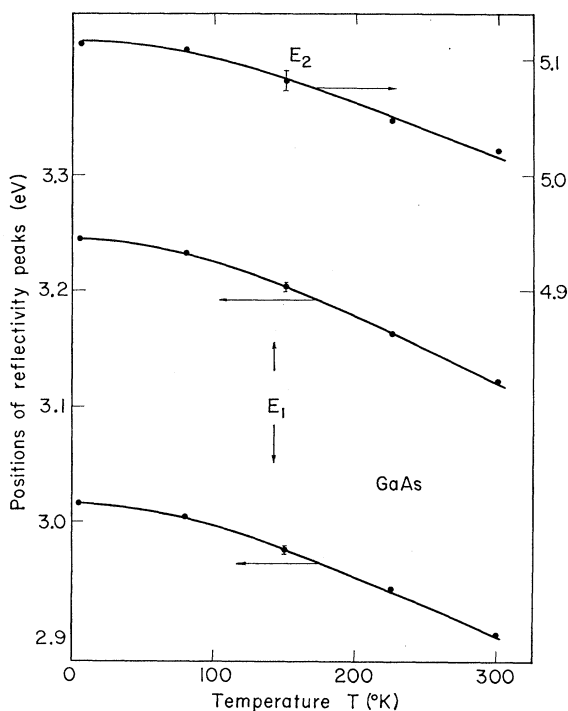


FIG. 10. Temperature shifts of the  $E_1$  doublet and the major  $E_2$  reflectivity peak of GaAs.

$X_5 \rightarrow X_1$  transitions at an energy between  $\Sigma_2 \rightarrow \Sigma_1$  (4-5) and  $\Delta_5 \rightarrow \Delta_1$  (4-5) transitions. We cannot recognize any such structure in all our spectra. This suggests that either  $X_5 \rightarrow X_1$  transitions are too weak or they are hidden in the broad  $\Sigma_2 \rightarrow \Sigma_1$  (4-5) peak.

The small  $E_2$  peaks have higher energies than the  $\Sigma_2 \rightarrow \Sigma_1$  (4-5) transitions. As seen from Fig. 10, they should correspond to transitions between the valence band (band 4) and the second conduction band (band 6). There is some ambiguity in decomposing the small  $E_2$  structures, but we can unambiguously identify one peak in Ge, one in Si, three in InAs, InSb, and GaSb, and probably also three in GaAs. We then recognize that for all the III-V compounds, the spacing between two of the three peaks agrees quite well with the spin-orbit splitting of the  $\Delta_5$  level (see Table I). We, therefore, assign the doublet to 4-6 transitions along  $\Delta$  (close to  $X$ ).<sup>27</sup> The same transitions should give rise to only one reflectivity peak in Ge and Si, since the spin-orbit splitting along  $\Delta_5$  for these two elements is small.<sup>24,26</sup> Accordingly, the small  $E_2$  peak of Ge and Si should correspond to  $\Delta_5 \rightarrow \Delta_1$  (4-6) transitions. The remaining small  $E_2$  peak of the III-V compounds is possibly due to 4-6 transitions around  $\Sigma$  or in the region around  $X_5 \rightarrow X_3$  as suggested by pseudopotential calculation.<sup>28</sup> Such a peak did not show up in the spectra of Ge and Si pre-

<sup>26</sup> F. Herman, C. D. Kuglin, K. F. Cuff, and R. L. Kortum, Phys. Rev. Letters 11, 541 (1963).

<sup>27</sup> This assignment is also suggested by pseudopotential calculation for GaSb which shows two spin-orbit split peaks coming from 4-6 transitions along  $\Delta$  in the neighborhood of  $X$  (see Ref. 17).

<sup>28</sup> J. P. Walter (private communication).

sumably because of the slight difference in their band structures.

#### D. $E_1'$ Region

Our spectra, limited by the uv cutoff of the spectrometer, cover only part of the  $E_1'$  region in Si, Ge, GaSb, and InSb, and none in GaAs and InAs. The  $E_1'$  peaks are normally assigned to 4–6 transitions along  $\Lambda$  close to  $L$ .<sup>3,29</sup> Both  $\Lambda_3$  levels are spin-orbit split, but the splitting of  $\Lambda_3(6)$  is expected to be considerably smaller than that of  $\Lambda_3(4)$ .<sup>17,21</sup> We should, therefore, expect to see two doublets separated by the spin-orbit splitting of  $\Lambda_3(4)$ .

In Si, the spin-orbit coupling is small, and we have observed only one unresolved reflectivity peak as expected. In Ge, we can identify two peaks with a separation somewhat larger than the splitting of the  $\Lambda_3 \rightarrow \Lambda_1$  doublet. This suggests that the splitting of  $\Lambda_3(6)$  in Ge is very small, and the observed  $\Lambda_3 \rightarrow \Lambda_3$  transitions are closer to  $L$  than the  $\Lambda_3 \rightarrow \Lambda_1$  transitions. In InSb, where the spin-orbit coupling is larger, we have actually observed three peaks with the fourth one being cut off by our spectrometer. The spin-orbit splitting of  $\Lambda_3(4)$  derived from them is again somewhat larger than the splitting of the  $\Lambda_3 \rightarrow \Lambda_1$  doublet. The separation of the two closely overlapping peaks gives the spin-orbit splitting of  $\Lambda_3(6)$  near  $L$  (see Table II). In GaSb, we can observe only one doublet with a small splitting corresponding to the splitting of  $\Lambda_3(6)$ . The other doublet at higher energy should be outside the range of our spectrometer.

From the above description, we have seen that the consistency of our assignment of reflectivity peaks is remarkably good. For more quantitative discussion, one must, however, resort to pseudopotential calculations.<sup>1</sup> We have deduced from our spectra the spin-orbit splittings at various symmetry points in different crystals. The results are summarized in Table II.

We can also obtain from our spectra at various temperatures some information about the temperature dependence of the band structures. Figures 2–7 show that all the major reflectivity peaks shift to lower energies at higher temperatures. This temperature effect can be understood qualitatively from thermal expansion of crystal lattices and the Debye-Waller effect.<sup>30</sup> Expansion of a lattice should reduce the energy separation between bands. Lattice vibration at finite temperatures should decrease the effective core potential by the Debye-Waller factor, and, hence, decrease the splittings between bands.<sup>30</sup>

The temperature shift of a reflectivity peak is rather smooth and gradual. We have studied the temperature effect on GaAs in more detail. Figure 10 shows the temperature shifts of the  $E_1$  doublet and the major  $E_2$  peak of GaAs. The three curves behave similarly. We can deduce from these curves an average temperature co-

TABLE III. Average temperature shifts in unit of  $10^{-4}$  eV/°K between 80 and 300°K for the  $E_1$  doublet and the major  $E_2$  peak in the six crystals. Accuracy is  $\pm 0.4 \times 10^{-4}$  eV/°K.

	GaAs	GaSb	InAs	InSb	Ge	Si
$E_1$	-5.3	-4.5	-5.0	-4.4	-4.2	-2.2
$E_2$	-3.6	-4.1	-5.6	-3.6	-2.4	-2.2

efficient of  $dE/dT = (5.3 \pm 0.4) \times 10^{-4}$  eV/°K for the  $E_1$  doublet and  $(3.6 \pm 0.4) \times 10^{-4}$  eV/°K for the  $E_2$  peak in the temperature range between 80 and 300°K. The observed temperature shifts also fit well with the exponential dependence

$$\Delta E(T) \equiv E(T) - E(5^\circ\text{K}) = A e^{-B/T}$$

with, for example,  $A = 0.28$  eV,  $B = 320^\circ\text{K}$  for the  $E_2$  peak. In the other crystals, we have observed similar temperature dependence of the reflectivity peaks. We present in Table III the observed temperature coefficients of the  $E_1$  and the major  $E_2$  peaks for all the six crystals. Note that Si has a smaller temperature dependence than the other crystals, presumably because it has a higher Debye temperature.

As seen from our spectra, all the structures become sharper at lower temperatures. This is presumably due to reduction of lifetime broadening. In particular, the  $E_1$  peaks have been associated with hyperbolic excitons partly for this reason. There are also remarkable sharpening of  $E_2$  and  $E_1'$  peaks at low temperatures. It would be interesting to know whether exciton effects are also important in these transitions.

## V. CONCLUSION

We have demonstrated in this paper the superiority of wavelength-modulation spectroscopy. Our derivative spectra of the six semiconductors show clear improvement on the spectral resolution over other techniques. In particular, our low-temperature spectra give more clearly defined reflectivity peaks than either electroreflectance or thermoreflectance spectra. With available information about the band structures, the spin-orbit splittings, and similarities among the semiconductors, we can consistently assign all the observed reflectivity peaks to proper critical transitions between bands. Values of spin-orbit splittings at various symmetry points can then be deduced. Results agree well with simple theoretical estimates.

Our measurements at various temperatures also yield valuable information about the temperature dependence of the band structures. As predicted by qualitative argument, all the reflectivity peaks shift to higher energies at lower temperatures. The structures in the spectra generally become much more pronounced at lower temperatures. Sharpening of the  $E_1$  peaks at low temperatures is particularly striking and can be explained in terms of reduction of lifetime broadening of the hyper-

<sup>29</sup> M. Cardona, in *Proceedings of the Seventh International Conference on the Physics of Semiconductors, Paris, 1964* (Dunod, Paris, 1964), p. 181.

<sup>30</sup> J. P. Walter, R. R. L. Zucca, M. L. Cohen, and Y. R. Shen, *Phys. Rev. Letters* **24**, 102 (1970).



bolic excitons associated with  $\Lambda$ . Whether the exciton effect is also important in the other transitions remains to be investigated.

To help us make sure that our assignment of reflectivity peaks is correct, measurements on samples under uniaxial stress should be performed. That a stress can be exerted on the sample without much complication is another advantage of the wavelength-modulation scheme. The pressure dependence of the reflectivity spectrum should also yield valuable information about

hyperbolic excitons associated at various symmetry points.<sup>31</sup>

#### ACKNOWLEDGMENTS

We would like to thank M. L. Cohen, J. P. Walter, R. Cahn, and C. Y. Fong for many helpful discussions, and M. P. Klein for technical help. This work was done under the auspices of the U. S. Atomic Energy Commission.

<sup>31</sup> E. O. Kane, *Phys. Rev.* **178**, 1368 (1969).

## Infrared Cyclotron Resonance and Related Experiments in the Conduction Band of InSb†

E. J. JOHNSON AND D. H. DICKEY

*Lincoln Laboratory, Massachusetts Institute of Technology, Lexington, Massachusetts 02173*

(Received 29 August 1969)

We present a comprehensive study of the conduction band of InSb. Experimental observations of fundamental cyclotron-resonance transitions involving the lowest Landau levels and both spin states are reported over a range of magnetic fields from 5 to 35 kG. Additional transitions involving impurities, phonons, cyclotron-resonance harmonics, and spin flip are also observed. The fundamental cyclotron resonance and the spin-flip cyclotron resonance, together with the spin-resonance results of Isaacson, are analyzed in terms of a nonparabolic band theory involving interactions with the six valence bands and allowing the possibility of interactions with more remote bands. A good fit to the nonparabolic band theory is obtained when one is careful to remove effects due to impurities and the electron-phonon interaction. A band-edge effective mass of  $0.0139m$  and a band-edge  $g$  factor of  $-51.3$  are obtained. An analysis using these values shows that remote band interactions contribute to the value of either the mass or  $g$  factor or both by an amount on the order of 10%. The transition energies for cyclotron-resonance harmonics, spin-flip transitions, phonon-assisted cyclotron resonance, and spin resonance as a function of Fermi level have been calculated and give a good fit to the data. This confirms the identification of these transitions and shows that the nonparabolic theory gives the magnetic energy levels correctly to energies as high as 60 meV. A value of 24.4 meV is found for the LO phonon energy. The existence of the phonon-assisted cyclotron resonance is explained on the basis of the mixing of Landau levels by the electron-phonon interaction. The strength of the cyclotron-resonance harmonics is not satisfactorily explained, although several possible mechanisms are proposed. An  $H=0$  electron-energy dispersion relation and other related band properties are deduced from the magnetic field results and compared with other experiments.

### I. INTRODUCTION

FOR some time there has been a great need for the determination of the precise location of the conduction-band energy levels in InSb, both with and without a magnetic field. Experiments involving excitons,<sup>1</sup> polarons,<sup>2-4</sup> interband absorption,<sup>5</sup> and Raman

scattering<sup>6</sup> have been performed. The analysis of these experiments depends critically upon the precise location of the conduction-band energy levels.

We report here a comprehensive study of the conduction band of InSb using infrared cyclotron resonance. We have employed improved techniques to obtain sharp lines with well-resolved structure. Our fit of nonparabolic theory to the experimental results takes into account band interaction effects and provides a precise determination of the band-edge effective mass and effective spin  $g$  factor. We identify transitions involving cyclotron-resonance harmonics and transitions involving an LO phonon. From these results, we obtain a measure of the zone center LO phonon energy. A better understanding of the fine structure is

† Work sponsored by the Department of the Air Force.

<sup>1</sup> E. J. Johnson, *Phys. Rev. Letters* **19**, 352 (1967).

<sup>2</sup> E. J. Johnson and D. M. Larsen, *Phys. Rev. Letters* **16**, 655 (1966); also D. M. Larsen and E. J. Johnson, in *Proceedings of the International Conference on Physics of Semiconductors*, Kyoto, 1966, p. 443 (unpublished).

<sup>3</sup> D. H. Dickey, E. J. Johnson, and D. M. Larsen, *Phys. Rev. Letters* **18**, 599 (1967); see also C. J. Summers *et al.*, *Phys. Rev.* **170**, 755 (1968).

<sup>4</sup> D. H. Dickey and D. M. Larsen, *Phys. Rev. Letters* **20**, 65 (1968).

<sup>5</sup> C. R. Pidgeon and R. N. Brown, *Phys. Rev.* **146**, 575 (1966).

<sup>6</sup> R. E. Slusher, C. K. N. Patel, and P. A. Fleury, *Phys. Rev. Letters* **18**, 77 (1967).